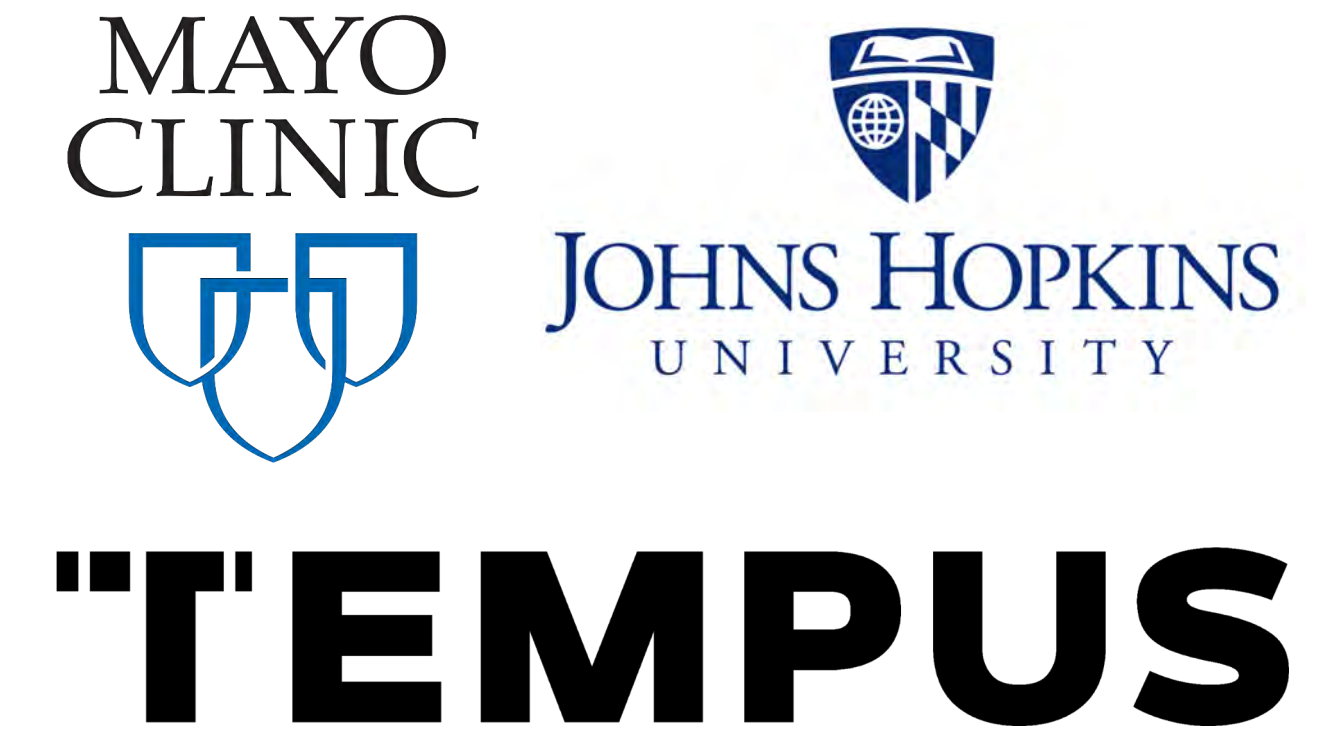


Multimodal Profiling of Biliary Tract Cancers Detects Potentially Actionable Biomarkers and Differences in Immune Signatures Between Subtypes



Kabir Mody¹, Nilo Azad², Prerna Jain³, Sherif M El-Refai³, Rachna T Shroff⁴, R Katie Kelley⁵, Anthony B El-Khouiery⁶, Denise Lau³, Gregory B Lesinski⁷, Mark Yarchoan²

¹Mayo Clinic, Jacksonville, FL, USA, ²Johns Hopkins University, Baltimore, MD USA, ³Tempus Labs Inc, Chicago, IL, USA, ⁴Division of Hematology and Oncology, Department of Medicine, University of Arizona Cancer Center, Tucson, AZ, USA, ⁵The University of California, San Francisco Medical Center, San Francisco, CA, USA, ⁶USC Norris Comprehensive Cancer Center, Los Angeles, CA, USA, ⁷Emory University School of Medicine, Winship Cancer Institute, Atlanta, USA

INTRODUCTION

Biliary tract cancers (BTC) are increasingly subtyped by molecular alterations, but little is known about the relationship between gain-of-function mutations and the RNA transcript expression of immune-related pathways.

Here, we investigate the relationship between the mutational landscape and immune-related RNA signatures of different BTC subtypes, including intrahepatic (IH) vs. extrahepatic (EH) cholangiocarcinoma and gallbladder (GB) cancer.

METHODS

From over 1500 BTC records, only records with matched RNA and clinical data (n=454) from the Tempus deidentified database were selected for DNA profiling and RNA signature analysis. IH, EH, and GB cancer data from any stage, treatment status, or tumor site was included.

Association analysis included tumor mutational burden (TMB), RNA-estimated immune infiltrate proportions, and established immune-related gene expression scores: cytolytic activity (CYT)¹, neoadjuvant response (NRS)² immuno-predictive (IMPRES)³, T cell inflamed gene expression profile (GEP)⁴, BMS inflammatory⁵ and dendritic cell (DC) score⁶.

Table 1. Clinical Characteristics of Cohort

Characteristic	Overall	EH	GB	IH	P-Value	
Total n	454	35	153	267		
Gender, n (%)	Female	268 (59.0)	16 (47.1)	109 (71.2)	143 (53.6)	0.001
	Male	188 (41.0)	18 (52.9)	44 (28.8)	124 (46.4)	
Age at biopsy, median [Q1, Q3]	Overall	66.0 [58.8, 72.6]	67.6 [59.3, 73.1]	66.7 [60.6, 75.0]	65.6 [58.0, 71.2]	
	Stage 1	10 (4.6)	2 (9.5)	2 (2.0)	6 (6.1)	0.072
Stage at RNA biopsy, n (%)	Stage 2	12 (5.5)	3 (14.3)	1 (1.0)	8 (8.2)	0.055
	Stage 3	27 (12.3)	2 (9.5)	18 (18.0)	7 (7.1)	
	Stage 4	171 (77.6)	14 (66.7)	79 (79.0)	77 (78.6)	
ECOG, n (%)	0	86 (40.2)	5 (31.2)	26 (41.3)	55 (40.7)	
	1	104 (48.6)	8 (50.0)	33 (52.4)	62 (45.9)	
	2	19 (8.9)	2 (12.5)	3 (4.8)	15 (11.1)	
	3	5 (2.3)	1 (6.2)	1 (1.6)	3 (2.2)	
Smoking history, n (%)	False	316 (69.6)	26 (76.5)	111 (72.5)	179 (67.0)	0.081
	True	138 (30.4)	8 (23.5)	42 (27.5)	88 (33.0)	
Leucovorin pre-biopsy, n (%)	False	431 (94.9)	34 (100.0)	147 (96.1)	250 (93.6)	0.349
	True	23 (5.1)	6 (3.9)	6 (3.9)	17 (6.4)	
Oxaliplatin pre-biopsy, n (%)	False	420 (92.5)	33 (97.1)	146 (95.4)	241 (90.3)	0.17
	True	34 (7.5)	1 (2.9)	7 (4.6)	26 (9.7)	

Table 1. Clinical characteristics of data records were analyzed in the overall cohort and compared across BTC subtypes. An enrichment for female records with GB was observed and consistent with elevated risk for females with the GB subtype.

SUMMARY

BTC subtypes exhibit diverse DNA alterations, RNA inflammatory signatures, and immune markers. Potentially actionable biomarkers were identified in a sizable portion of the cohort and varied significantly between subtypes. Notably, **gallbladder samples were relatively more inflamed based on RNA signatures and classical immune biomarkers, including PD-L1 and TMB.** These results provide guidance for targeted therapy development and support the use of multimodal immune profiling for BTC.

RESULTS

Figure 1. CYT and NRS RNA Biomarker Signatures Significantly Differ Between GB and IH BTC Subtypes

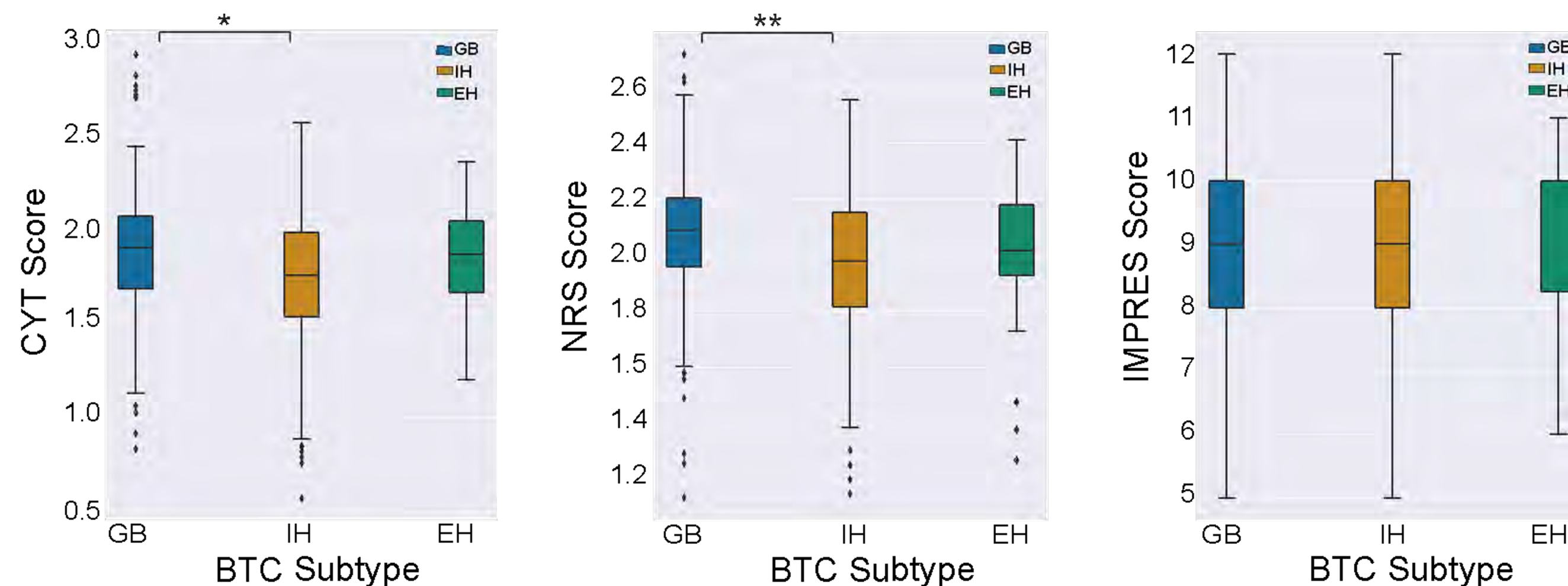


Figure 1. RNA signatures, including cytolytic activity (CYT), neoadjuvant response (NRS) and immuno-predictive (IMPRES) scores, compared across BTC subtypes (n=454). RNA signature analyses revealed a higher expression of immune-related pathways in GB than IH (* $P < 0.01$, ** $P < 0.001$) with no differences in comparison with EH.

Figure 2. Gene Mutation Associations with Tumor Mutational Burden, Immune Infiltrate Proportions and RNA Biomarker Signatures

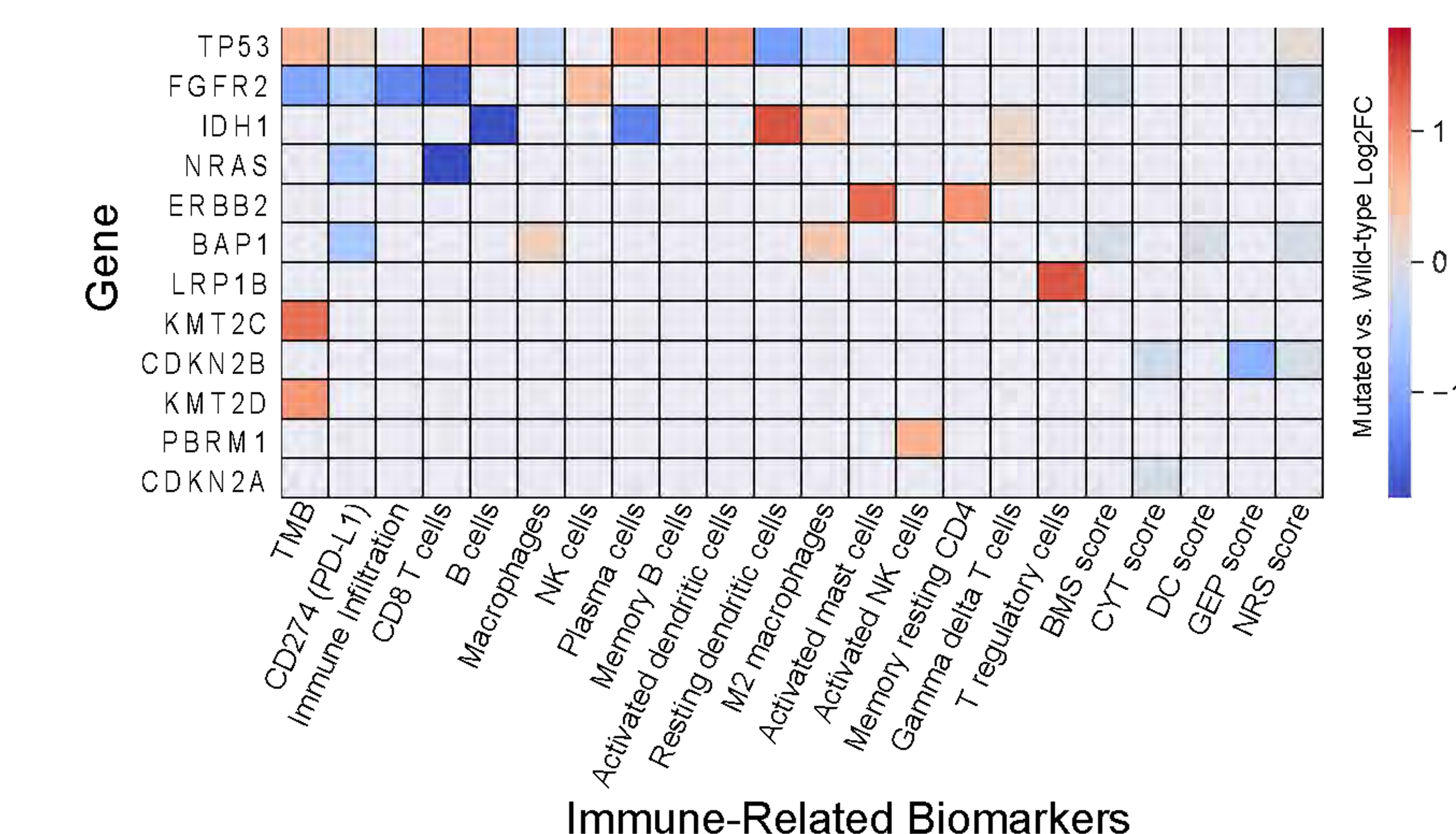


Figure 2. Gene-biomarker associations across patients with matched DNA, RNA, and clinical data (n=296). Colored blocks in the heatmap indicate significantly correlated gene-biomarker pairs (log-fold change) in mutant versus wild-type groups (Mann-Whitney U-test).

Figure 3. Higher PD-L1 Expression and Tumor Mutational Burden Are Significantly Associated with GB compared to the IH BTC Subtype

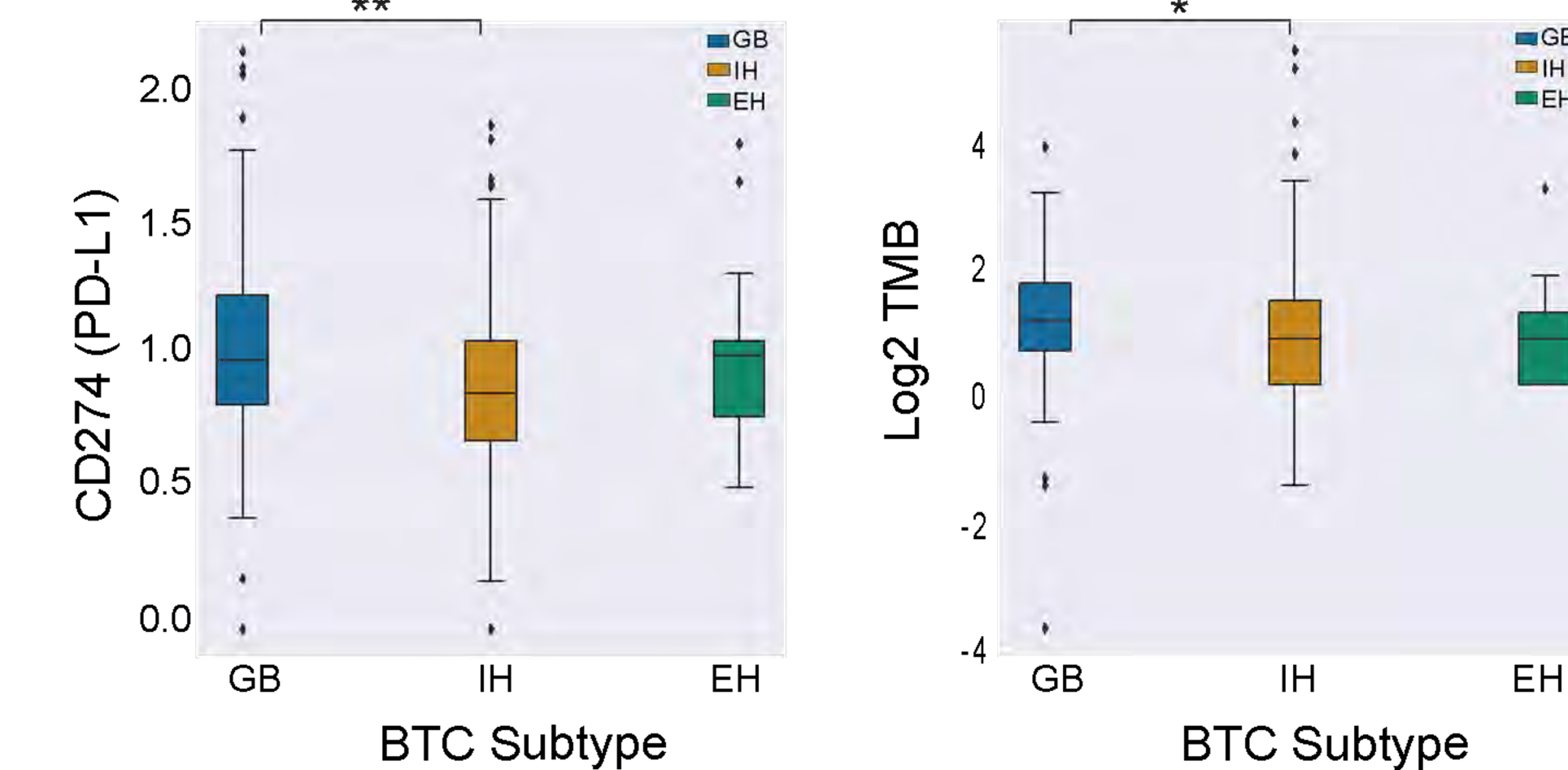


Figure 3. CD274 (PD-L1) RNA expression and tumor mutational burden (TMB) compared across BTC subtypes (n=296). Both IO biomarkers analyses revealed a higher expression of PD-L1 and higher TMB in GB than IH (* $P < 0.01$, ** $P < 0.001$) with no differences in comparison with EH.

Figure 4. Mutational Frequency Differs Across BTC subtypes with Distinct Clusters Based on Driver Mutation Status

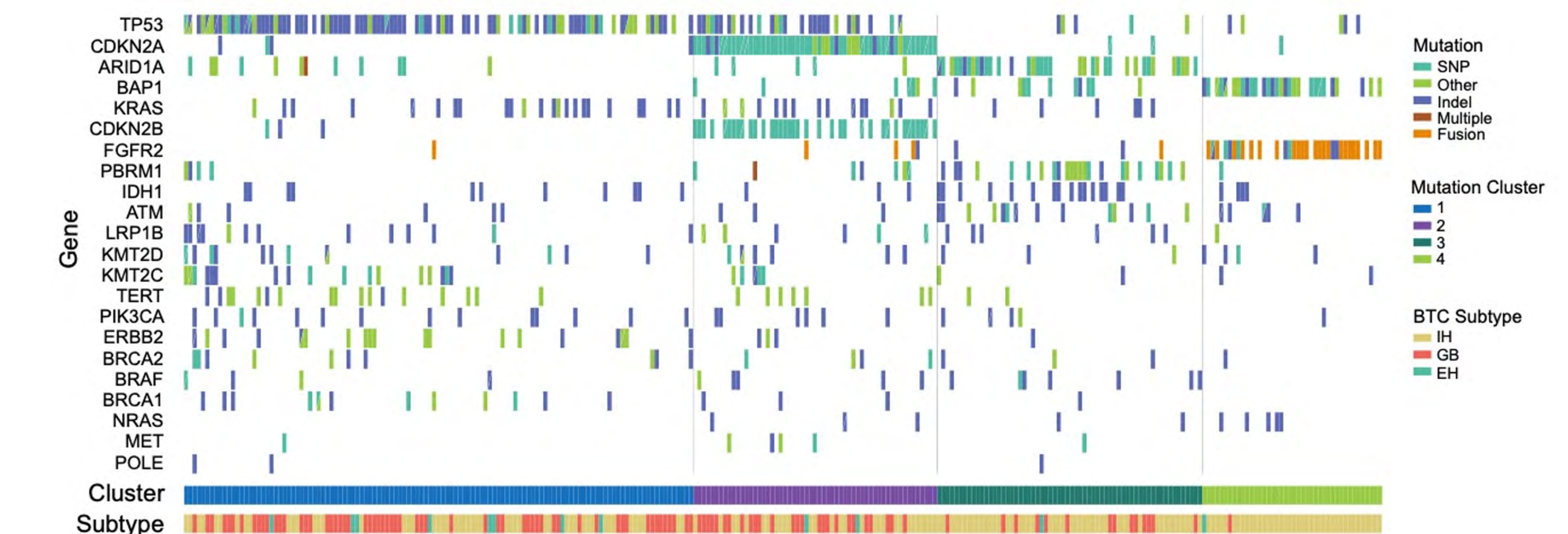


Figure 4. Mutational frequency across BTC subtypes detected alterations in *TP53* (45.9%), *CDKN2A* (22.6%), *ARID1A* (18.9%), *BAP1* (17.2%), *KRAS* (14.9%), *CDKN2B* (13.2%), *PBRM1* (12.5%), *IDH1* (11.8%), *TERT* (9.5%), *KMT2C* (9.1%) and *LRP1B* (8.8%), along with *FGFR2* fusions (10.1%). Four distinct clusters based on driver mutation status were detected, with cluster 4 predominately associated with *FGFR2* and *BAP1* mutations in IH. Indel, insertion/deletion; SNP, single-nucleotide polymorphism.